Fermilab Proposal # 703

June 1981

ELECTRON-PROTON COLLISIONS AT FERMILAB

E. Blackmore[m], R.K. Carnegie[a], S. Conetti[f], M. Dixit[i], K.M. Edwards[a], P.G. Estabrooks[f], J. Feltesse[j], J. Fraser[b], W.R. Frisken[n], L. Hand[c], C.K. Hargrove[i], R.J. Hemingway[f], P. Hobson[i], N. Isgur[l], D. Johnson[e], A. Leveque[j], J.F. Martin[f], J. McKeown[b], A. McPherson[a], F. Merritt[d], H. Mes[i], F. Mills[e], R. Orr[f], P. Padley[n], P. Patel[h], J. Pilcher[d], J.D. Prentice[l], A. Ruggiero[e], H. Schneider[b], S. Schriber[b], R. Servranckx[k], A. Skuja[g,h], M. Spiro[j], D.G. Stairs[h], J.-C. Thevenin[j], L. Turnbull[n], J. Trischuk[h], M.K. Wong[l], T.-S. Yoon[l]

a)Carleton University
b)Chalk River Nuclear Lab
c)Cornell University
d)Enrico Fermi Institute
e)Fermilab
f)Inst. of Particle Phys.
g)University of Maryland
h)McGill University
i)National Research Council
j)Saclay
k)U. of Saskatchewan
l)U. of Toronto
m)TRIUMF
n)York University

spokesperson: W.R. Frisken, Department of Physics, York University,
4700 Keele Street, Downsview, Toronto, Canada M3J 1P3
416-667-3963

I. Prologue

In September 1980 the CHEER (Canadian High Energy Electron Ring) Group submitted simultaneously to the Canadian government and to the Program Advisory Committee of Fermilab our Blue Book: "A Feasibility Study for an Electron Ring at a High Energy Proton Accelerator"[1].The study concentrated on the idea of building a 10 GeV polarised electron (and positron) ring tangent to the Tevatron and indeed succeeded in proving the scientific merit of such a project, demonstrating its technical feasibility, and carefully estimating its cost.

In the interim there have been developments on several fronts. The most encouraging one is an emerging realisation in the United States and Canada that an ep collider constitutes one of the great opportunities for North American leadership in the physics of the 1980's and 1990's. For a very modest cost, such a facility would provide access to unique and exciting physics issues unattainable elsewhere, and it would do so well ahead of any foreseeable competition. This growing awareness has been sparked in part by the CHEER project (and by the parallel effort in the U.S. centred at Columbia), so in this regard we consider our project to have already been successful. We have been less successful in achieving funding for the project, but remain committed to continue our studies of ep physics into the next year. The purpose of pursuing these studies is to elaborate and refine the discussions of the Blue Book to the point that, when funding for the project is found, engineering design can begin almost immediately. Thus the aims include preparation of a detailed and sophisticated ep Monte Carlo, testing and refining an ep detector by tracking the Monte Carlo events through various hypothetical detectors, and solving the remaining machine problems left open by the feasibility study. We expect this year of research to bring our understanding of ep physics to a new level of sophistication that will provide significant new insights into machine and detector design.

In the meantime, we would like to elevate our submission to the Fermilab Program Advisory Committee from an "information package" to a proposal in order to stimulate and focus the discussions on attaining high energy ep collisions in North America. We believe that the Blue Book remains an adequate basis for such a proposal; the purpose of this note is consequently threefold:

1) to "formally" propose an ep collider experiment at Fermilab,

2) to update briefly the discussion of the Blue Book with some of our findings of the last six months, and

3) to provide a sketch of the actual initial experiments we envision for the collider facility.

It should be emphasized that the studies in which we are now engaged will be much more definitive on points 2) and 3) than this brief proposal can or is intended to be. We would also like to stress that we welcome the parallel initiatives being made by the proponents of P659 [2]; we believe that ep physics provides an outstanding opportunity to North American high energy physics and that all who wish to pursue it should do so as vigorously and co-operatively as possible.

II. An Update on the Blue Book

Since publication of the Blue Book a number of topics have already been subjected to further examination and refinement. While these studies are ongoing, we will review here the main areas in which further progress has been made. Aside from a better understanding of the radiative corrections in an ep collider, there have been no major developments in Chapter III (The Physics Motivation) of the Blue Book; this section will therefore deal entirely with brief updates on Chapters IV (The Machine) and V (The Detector).

A. The Machine

The preliminary design of a polarised 10 GeV electron storage ring and injector, which could be located at straight section DØ of the Fermilab Tevatron, has now been completed based on the work reported in the Blue Book. Particular attention has been paid to the Tevatron geometry, a provision for a bypass, and polarisation optimisation. The elements of this design are summarised in the following brief descriptions.

1) The Linac

A 300 MeV linear accelerator has been optimised for both electron and positron beams. The accelerating structure uses disk-and-washer cavities for two basic reasons: 1) this structure has a very high efficiency for converting rf power into useful beam power and 2) it has a very high coupling constant. The high coupling constant means tanks of up to 7 metres can be built with only one rf coupling port.

The accelerator comprises four tanks with a removable positron target located between tanks 1 and 2. Each 6.2 m long tank (including the co-axial coupling cavity) requires 11.6 MW of peak rf power at 2867.67 MHz to establish an average accelerating gradient of 12.2 MeV/m. Four 25 MW klystrons drive the accelerator, one for each tank. The beam bore-hole diameter is 2 cm and the outer diamter of the structure is 20 cm. The total length of the accelerator from the 100 kV gun to the end of the accelerator structure is 29.1 m.

In the electron mode, 60 mA of electrons are accelerated for 0.33μs after 3.3μs of rf field risetime for the structure. Operation at 15 Hz allows the main ring to be filled in ∿3 seconds. In the positron mode, 110 mA of electrons are accelerated for .33μs in the first tank after 2.6μs of rf field risetime. The 75 MeV beam impinges on a converter target producing 10 MeV positrons that are accelerated in the last three tanks of the accelerator. The extra rf power required for the electron mode is used to increase the average accelerating gradient in the last three tanks to 15.7 meV/m. Additional rf power is installed to provide an overdrive so that equilibrium fields can be established after 4.6 μs. A fast low- level rf control is required to reduce the output power by 15% at this time. In the positron mode the rf pulse for the last three tanks must start 2 μs before the rf pulse to tank 1. With operation at 25 Hz the main ring can be filled in ∿15 minutes with positrons.

2) <u>The Positron-Electron Accumulator Ring</u>

The principal requirements for the accumulator are that it be synchronous with CHEER, have adequate radiation damping and be capable of accumulation. We have chosen an energy of 300 MeV, a circumference equal to 19.75 m, one half the CHEER bunch spacing, and bend fields of 1.5 T with $n = 1/2$ to adjust the damping partition numbers ($Jx = Jz = 1/2\ J_E$).

The beam will be injected in horizontal betatron phase space by deflection of the central orbit (and the accumulated beam) to the proximity of a septum. Five turns are injected as the deflectors are turned off. For positrons, where the emittance is large (∿ πμm) the resulting beam will have large emittance, ∿ 100 πμm and a final damping of 60 - 100 msec will be required to fit into the booster.

For electrons the emittance is smaller, and damping during the normal 66 msec cycle is sufficient. The lattice should have zero or small dispersion and a low ($\sim$ 1 m) β_x value at the injection straight section to accommodate injection. Magnet-free regions are required at the 90^o horizontal phase position for injection kickers.

The injected beam is captured adiabatically with a 15.2 MHz 25 kV system. The rf turn-on should be in several phase oscillations, or $\sim$ 60 μs. The rf should not be turned off completely but only reduced to $\sim$ 5 kV during this process. After 66 msec the electrons will have damped to a bunch of length 1.2 nanoseconds. Bunch lengthening phenomena may limit the damping, so the next rf system has an acceptance of 5 nsec (201 MHz).

The design of the lattice can follow that of PIA[3)] in all details. The multiturn injection will make the horizontal aperture large; approximately 10 cm good field width and 5 cm height would be advisable. Sextupoles should be provided to make the chromaticity slightly positive.

3) The CHEER Booster

The booster is required to accept the accumulator bunches at 300 MeV and deliver them to CHEER at 2 GeV. A 15 Hz rapid cycling synchrotron similar to the Cornell electron synchrotron, or the Fermilab Booster or the Argonne Booster II offers the simplest solution. It also has the advantage of ease of operation during beam acceleration.

To be synchronous with CHEER, the length is chosen to be 98.75 metres, or the distance between 2 1/2 bunches in CHEER. Field strengths in the combined function magnets can reach 0.7 T. The lattice should include 3 m straight sections for injection, extraction, and rf and 1 m straight sections for injection and extraction kickers. It appears possible to do this with a bend radius of about 10 m. In order to avoid large β variations the phase advance per cell should be small.

A suggested lattice for one octant of the accelerator is FO(1.01 m) FDO(3 m)D, giving ρ = 10.61 m and B = .629 T. Then there should be 32 magnets of 2.08 metre length, 16 F and 16 D. If the phase change per octant is slightly above 90^o, then the k values can be ~ 1 and $\nu \sim 2.25$. The radiation loss is about .134 meV/turn and the horizontal emittance will suffer about 2.8 e-folding by radiation while damping a factor of 7 adiabatically. Longitudinally there will be about an e^{-10} reduction in phase space area. Rf requirements at 201 MHz are about 5 kV to match the bunch from the accumulator, 40 kV to keep up with the biased sinusoidal magnetic field, and 144 kV to replenish the radiation loss at the end of the cycle.

Aperture requirements in the magnet system are modest for the beam itself, about 20 mm x 5 mm. On the other hand instability control will pose a more serious requirement. Closed orbit deviations due to magnet and survey errors will similarly add several mm to the aperture requirements. Because of the single bunch, injection kicker risetime requirements are modest.

4) The CHEER Lattice

The parameters of the CHEER main ring lattice (see Table 1) are chosen to optimise the luminosity and polarisation at an electron energy of 10 GeV. The Tevatron proton beam will be circular in cross section with a radius ($\sigma_x = \sigma_z$) of 0.15 mm, so the electron beam must have similar transverse dimensions. The length of the proton bunches dictates that the β_X^* of the electron beam be $\gtrsim$ 0.3 m. It follows that the horizontal emittance of the electron beam should be approximately $\sim 3 \times 10^{-8}$ m rad. These factors constrain the bending radius of the ring to about 100 m. The circumference of the lattice is not so constrained and is amenable to changes of the order of at least 10 - 15%.

Table 1

Canadian High Energy Electron Ring

MACHINE PARAMETERS

Pre-Injector	300	MeV LINAC
Accumulator	300	MeV
Injector	2	GeV SYNCHROTRON
Storage Ring	10	GeV
Filling Time	3	seconds for e^-, 15 minutes for e^+
Electrons per bunch	10^{11}	

Lattice Characteristics at 10 GeV		
Circumference	∿ 2000	m
Bend Radius	∿ 90	m
Polarisation	$\gtrsim$ 75%	
Polarisation Time	∿ 10	min
Gross Radius	∿ 160	m
2 straight sections	∿ 500	m each
64 cells, FODO, 90^o phase advance		
Momentum Compaction α	.0016	
Emittance $\varepsilon_x/\varepsilon_z$	.021/.0012	10^{-6} m rad. (no coupling)
β_{max}	23	m
η_{max}	0.73	m

RF Characteristics

Installed RF power	3.1 MW (4.8 MW with wigglers)
Radiated RF power	1.5 MW (2.3 MW with wigglers)
RF frequency	804 MHz
Radiation loss/turn	12.5 MeV (19.3 MeV with wigglers)

Intersection Region

Free space for detector	13 m
β_x^*/β_z^*	0.3/0.3
σ_x / σ_z	.08mm/.02mm (no coupling)
Crossing Angle	0^o
Beam beam tune shift	$\Delta\nu_p$ 0.0018 $\Delta\nu_e$ 0.0345
Dispersion η^*/η'^*	0./0.
Luminosity	$0.2\text{x}10^{32}\text{cm}^{-2}\text{s}^{-1}$ or $0.4\text{x}10^{32}$ with coupling 0.5 (assuming for the Tevatron ε(95%)=.026 mm mrad, β_p^*=5m, $1.4\text{x}10^{11}$ protons/2m long bunch, 159 bunches)

The main ring is approximately oval in shape. It is composed of two bending arcs connected on one side by a straight section and on the other by the low-beta interaction-region (IR) insertion. The IR has a bypass at $\pm$ 100m and polarisation rotators at $\pm$ 150m. Each bend arc is composed of 32 identical cells of the form:

QD - B - QF - B - QD

where QF (QD) is a radially focussing (defocussing) quadrupole, and B is a dipole. The length of each such cell is 13 metres. At each end of the two arcs are located two dispersion-suppressing cells similar in structure to the above cells, but containing smaller bends. The achromatic straight section contains the rf cavities, the injection system, and wiggler **magnets**. This section is composed of QD - QF - QD cells, each having a phase advance of 90°.

The low-beta IR insertion has the following structure (symmetric about IP):

IP - B - QF - QD - B - B - QF - QD B - QF - QD - SR

where IP denotes the interaction point, and SR a combination of dipoles and quadrupoles that rotate the spin to give both positive and negative helicities at the interaction point, where 13 m are available for the detector. The dispersion generated by the dipoles in the insertion region and in the spin rotator is controlled so that the beam is achromatic at the IP and at the ends of the spin rotator.

5) The CHEER RF System

The lattice design gives an energy loss per turn of 12.5 MeV to be compensated by the rf system. The choice of frequency is a compromise between quantum lifetime, shunt impedance and the availability of a power source. With 10^{11} electrons/bunch in CHEER, higher order mode losses are not expected to be a serious problem. The chosen frequency of 804 MHz is somewhat higher than is customary in storage rings but there are several advantages: the structures are physically smaller and the higher power densities are easily accommodated with a bi-periodic pancake-coupled structure operated in the $\pi/2$ mode, and only one tuner is required for tuning. The beam hole has a diameter of 9 cm which is sufficient to give 1.4% electric coupling between cells with a shunt impedance of 26 MΩ/m. Seven klystrons of modern design having 300 kW each will be used to drive the fourteen 9-cell structures; the field gradient will be a modest 1 MV/m at this frequency. Finally, an installed peak voltage of 24 MV operating at a synchronous phase of 151^{o} will assure a quantum lifetime of greater than 10 hours.

B. The Detector

A detailed conceptual design of the CHEER detector was given in the Blue Book, and is shown in Figure 1. Our aim has, from the beginning,been to produce a complete detector, capable of extracting all of the rich physics made accessible by high energy ep collisons. In any event, the detector capability required to measure the charged current ($ep \rightarrow \nu X$) cross section is considerable, and the elaboration required to change a competent charged current detector into a "do-all" detector seems to be relatively modest.

The high centre-of-mass energy ($s = 40{,}000\ GeV^2$) of CHEER often produces events with 40 secondary particles, and these are spread over a large range of momenta. The heart of the detector must therefore be a high resolution magnetic spectrometer, capable of handling these complex events with minimal ambiguity. Our design is based on an atmospheric pressure TPC (the optimal detector for multiple track reconstruction since it measures many three dimensional points on each track) plus several planes of drift chambers in the downstream proton direction. Such an atmospheric pressure (and hence low drift voltage) TPC would be modelled on the TPC which has been successfully taking data for some time at TRIUMF. Planar and cylindrical PWC's are added for triggering purposes, and a magnetic field of 2 Tesla is provided by a thin super-conducting solenoid. An electromagnetic calorimeter

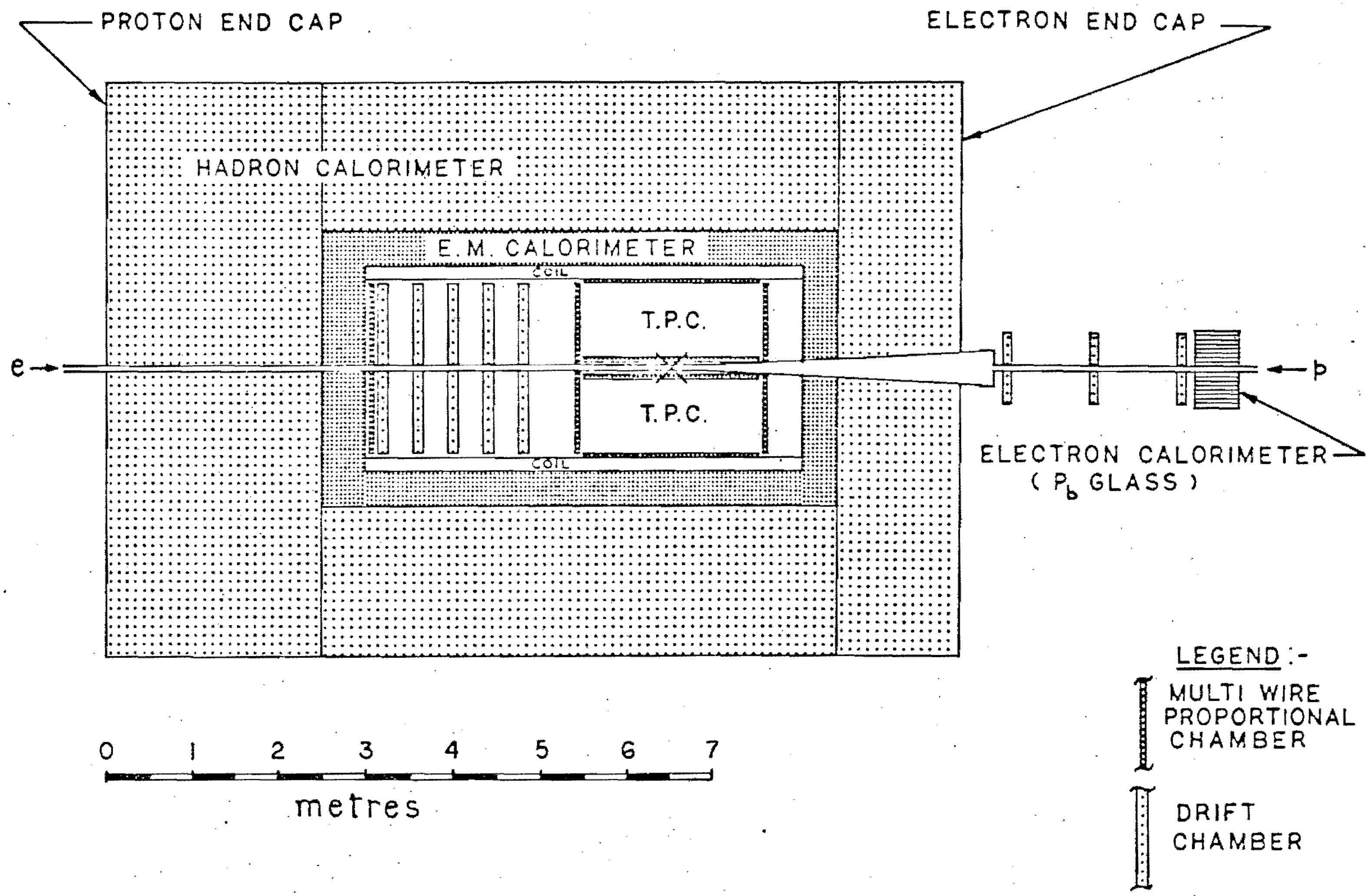

Figure 1: a schematic of the CHEER detector

almost completely surrounds this magnetic spectrometer. For charged current events ($ep \rightarrow \nu X$), it must guarantee the absence of an electron (as in $ep \rightarrow eX$) at the appropriate x and Q^2; it should also pick up the π^o photons associated with the hadron vertex, as well as hard radiative photons. The electromagnetic calorimeter is thus required to have nearly 4π solid angle coverage, with good spatial and energy resolution. In our design it consists of a fine sampling array of lead and plastic scintillator. A hadron calorimeter, in turn, surrounds this electromagnetic calorimeter. It picks up neutrons and K_L^o's, and it takes over from the magnetic spectrometer to measure energies for charged hadrons above 25 GeV. It also assists the electromagnetic calorimeter in electron identification, and it tracks and identifies muons via drift chambers between its coarser outer layers. It is thickest and most elaborately instrumented in the end cap in the downstream proton direction (called $\theta = 180^o$); everywhere it uses iron as a converter, so that it provides the return flux path for the magnetic spectrometer.

A useful approximation to the kinematics of ep collisions is obtained by idealising the initial state as a zero mass electron colliding with a free zero mass quark of momentum xP_p, and the final state as a zero mass lepton balanced by a zero mass "current jet" of hadrons of momentum P_J deflected $\pi - \theta_J$ from the proton direction. The lab system for such a collision is represented in figure 2. The ellipses are curves of constant x, while the almost vertical curves in the upper half plane are lines of constant Q^2 for the lepton, and the almost horizontal curves in the lower half plane are lines of constant Q^2 for the hadron current jet. Having chosen x and Q^2 one can immediately sketch in the four-momentum conserving vectors for $\vec{P}_L$ and $\vec{P}_J$. The figure shows such a pair of vectors for $x = 0.3$ and $Q^2 = 4000$ GeV^2.

The population of this kinematically allowed region with

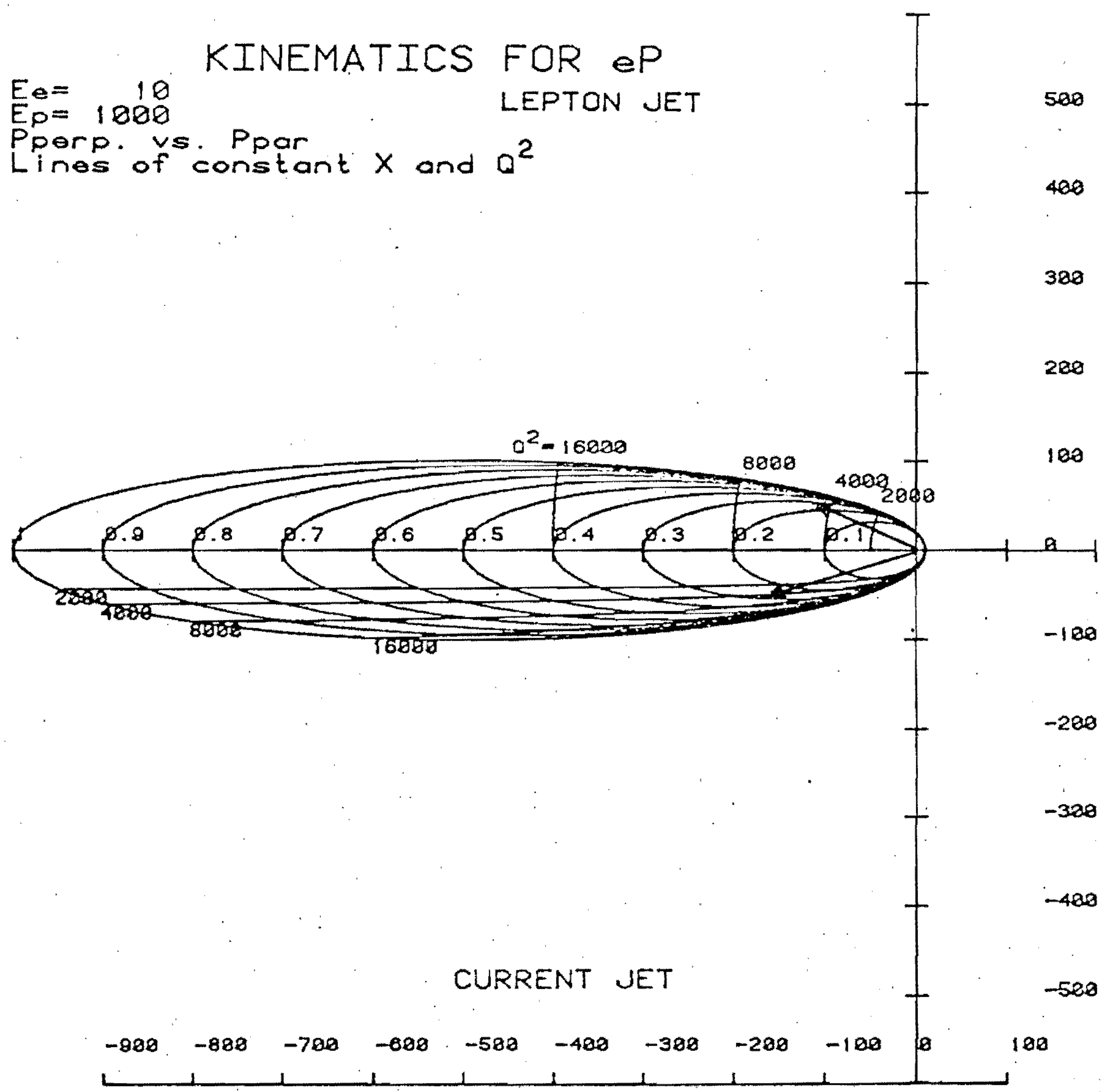

Figure 2: the kinematics of ep deep inelastic scattering with CHEER

events is determined by the dynamics of ep collisons, and is only known for $Q^2 < 100$ GeV^2. We show an extrapolation (via the standard theory) in Figure 3, which gives the numbers of charged current events ($ep \rightarrow \nu X$) expected in various regions of the (x, Q^2) plane for an initial run of integrated luminosity 4×10^4 nb^{-1} (corresponding to, for example, 1000 hrs at a luminosity of 10^{31} cm^{-2} sec^{-1}). In this figure Q^2 has been scaled to Q^2/s, so that lines of constant $y = \frac{Q^2}{sx}$ emanate from the origin with slope y, and the predictions can be given in xy bins. This charged current event distribution is, in the standard theory, completely determined by the structure functions $F_i(x,Q^2)$; from the display of Figure 3 it can be seen that even at $Q^2 = 10^4$ GeV^2 an initial run tests the structure functions for x above the kinematic limit of $Q^2/s = 0.25$, overlapping well with the region $x \lesssim 0.6$ where most of the quarks should be found.

It is instructive to examine the kinematics of charged current ($ep \rightarrow \nu X$) events in the same Q^2/s vs x plane, as shown in Figure 4. The dashed curves are lines of constant current jet energies, and the dotted curves are lines of constant current jet polar angle. The jet angles are expressed in deviations from 180°, so that $\Theta_J = \pi - .1$ means 100 mr from the original proton direction. Two points are immediately clear from comparison of Figures 3 and 4. The first is that a fast P_t trigger should be used with care, and at most in the end cap or bouchon ($\pi - \Theta_J \lesssim .25$), so as not to compromise the data at low x. The second is that a substantial part of the lower Q^2 regime consists of events in which the current jet axis lies within 100 mr of the beam pipe in the downstream proton direction.

Realisation of the full power of an electron-proton collider experiment as a probe of nucleon and quark structure, and of the structure of the electro-weak currents by which they interact with leptons, will require measurements over all the available range of Q^2. An important and obvious feature of this requirement is that good structure function measurements be made down to $Q^2 \sim 100$ GeV^2,

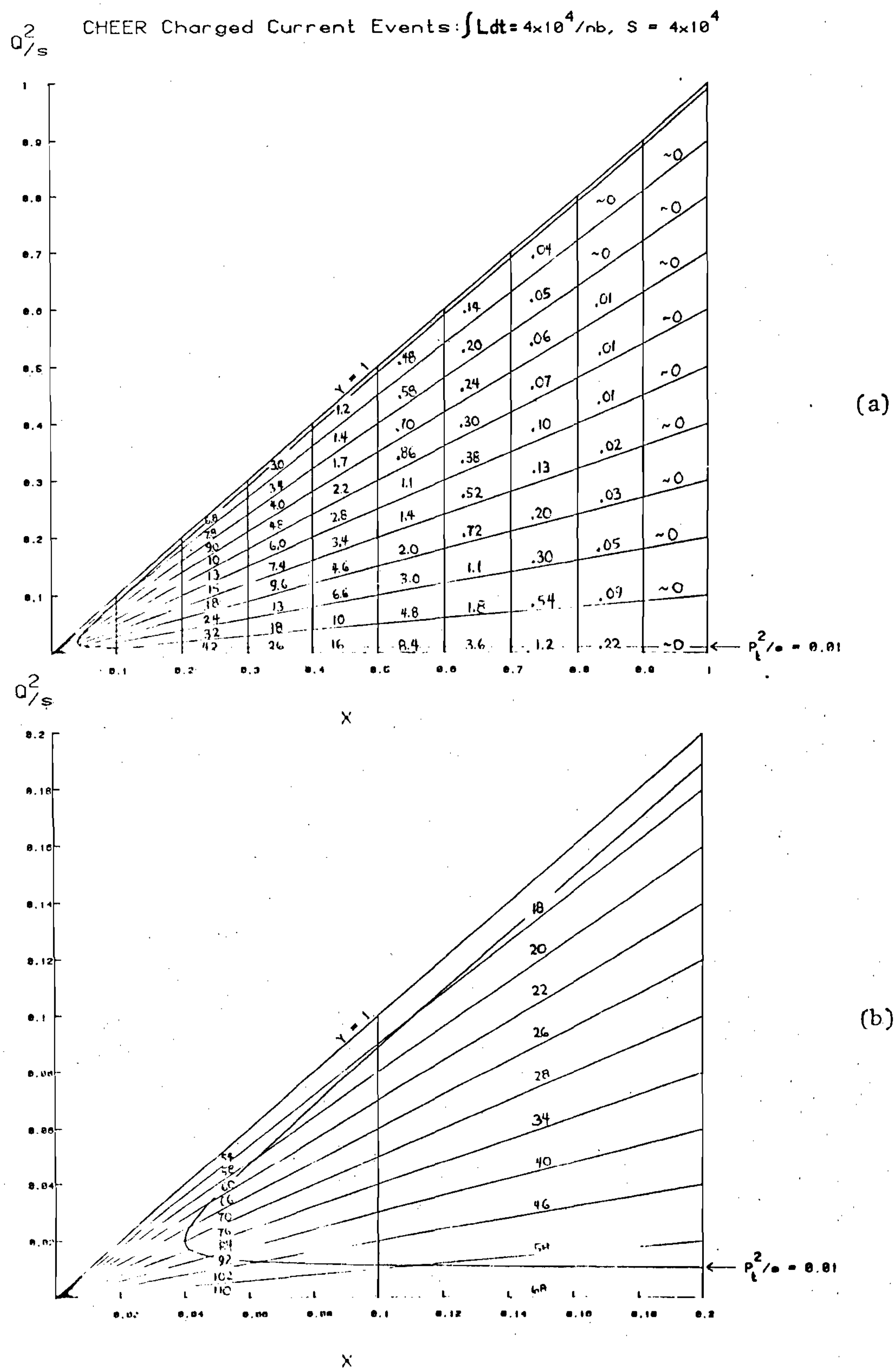

Figure 3: the distribution of charged current events in x and Q^2 for (a) x>0.2, and (b) x<0.2.

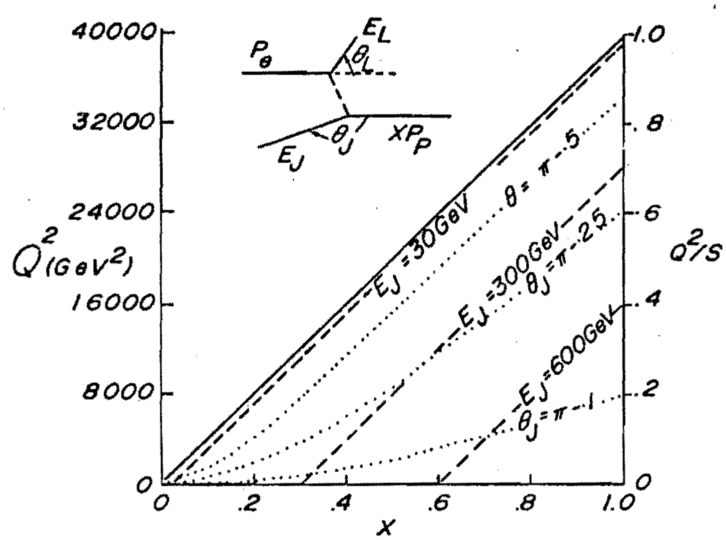

Figure 4: the kinematics of deep inelastic scattering in the (x,Q^2) plane

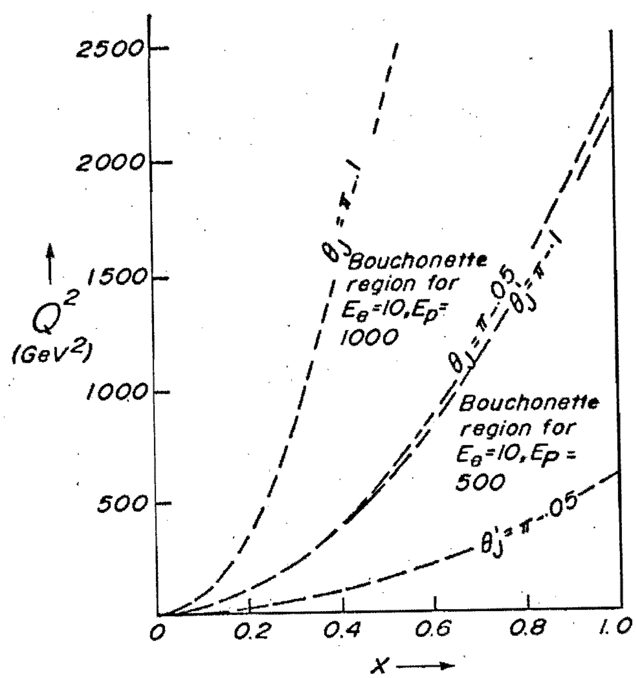

Figure 5: the variation of kinematics in the (x,Q^2) plane with E_p

to join onto the relatively shallow inelastic scattering measurements available from fixed target ep and μp experiments. We find that this is relatively easily accomplished for neutral current events ($ep \rightarrow eX$) which feature a well isolated wide angle final state electron of modest energy. However, charged current events ($ep \rightarrow \nu X$) must be determined by measuring a jet of high energy hadrons at small angles to the beam axis by calorimetry alone, since this is a topological regime for which the magnetic spectrometer is relatively weak. Although the energy resolution of calorimeters improves with increasing energy, there remains a problem due to the appreciable lateral spreading of individual hadronic showers in the hadron calorimeter.

The beam pipe for the exiting proton beam (and the entering electron beam) constitutes a hole in this calorimeter, but this can be made quite small (∿ 10 cm diam.). The dominant consideration is that realistic ep Monte Carlos (see below) show that the angular distribution of particles within the hadron jets has appreciable breadth. This is true of not only the current jet associated with the struck quark, but also the target fragmentation jet associated with the spectator di-quark system. The further spatial smearing which must result as the individual hadrons shower in the hadron calorimeter will lead to a degree of overlap of the two jets which will cause a considerable deterioration of performance in an important kinematical regime.

An approximate analysis technique suggested by Jacquet and Blondel[4] overcomes this problem in first order, but we will undoubtedly require a more complete separation. This can be accomplished by lowering the proton beam energy. The improvement in the capability of the bouchonette (for historical reasons we refer to the finely segmented part of the hadron calorimeter where $\pi - \Theta_J$ is less than 100 mr as the "bouchonette" region) at low Q^2 is shown in Figure 5, for a reduction of E_p from 1000 GeV to 500 GeV. Although there will be a loss of luminosity associated with lowering E_p (see p. 71 of the Blue Book for details), it appears that the low Q^2 charged current events will not be a problem if the bouchonette is finely segmented, and if some of the running time is spent with reduced proton energy. Running at lower E_p also has the advantage that it allows the Q^2 dependence of the structure functions to be directly disentangled from the y dependence of the measured cross sections by providing data at fixed x and y but varying Q^2. A final advantage of some running at lower E_p is that the region of the barrel-bouchon interface at $\Theta_J \sim \pi - .25$, where performance is bound to be somewhat poorer, will not always map into the same region in the (x, Q^2) plane.

It was an application of the preceding sort of qualitative analysis of the kinematics and dynamics for all the physics processes of interest in ep collisions that led to the schematic detector design of the Blue Book. However, evolution of such a schematic into the detailed design of a detector must proceed by an iterative process of specification and testing with Monte Carlo-simulated ep events.

The heart of the present ep Monte Carlo program is a quark fragmentation program adapted to ep collisions from the Lund Model.[5)] Events can be distributed in x and Q^2 according to any chosen structure function parametrization, and final state particles are produced by a QCD-motivated string-breaking model, which can operate with or without gluon jet production.

As a first step in the iterative design procedure we have superimposed drawings of a large sample of simulated events on a drawing of the schematic detector. In the version which produced Figures 6(a),(b),(c),(d),(e), and (f),all charged particles show tracks in the magnetic spectrometer region, electrons and photons are "detected" as soon as they enter the electromagnetic calorimeter, and hadrons are "detected" as soon as they enter the hadron calorimeter. The diamonds are scaled in area to represent electromagnetic shower energy, not shower size, and the triangles give a similar representation for

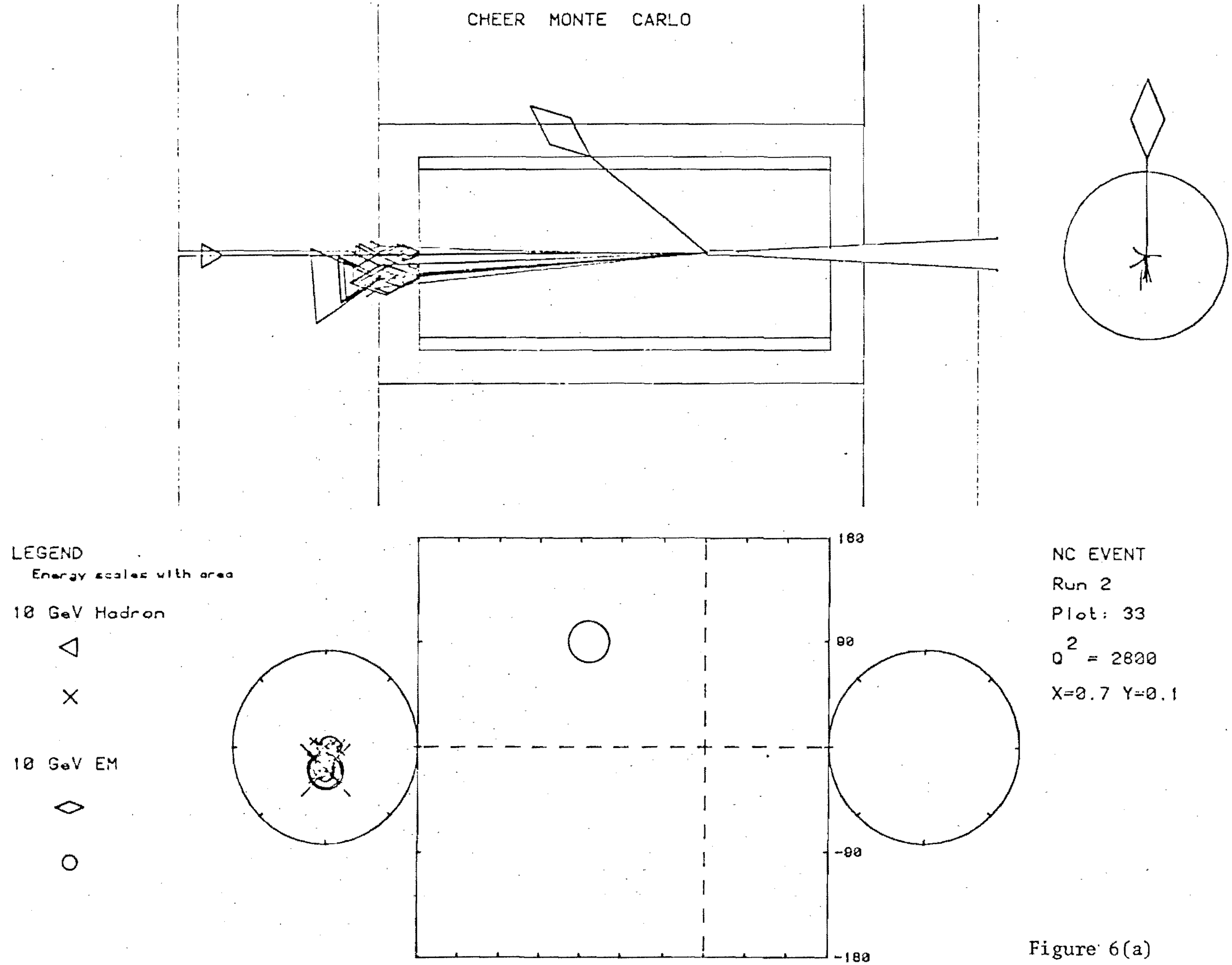

CHEER MONTE CARLO
LEGEND
Energy scales with area
10 GeV Hadron
10 GeV EM
180
90
-90
-180
NC EVENT
Run 2
Plot: 33
Q2 = 2800
X=0.7 Y=0.1

Figure 6(a)

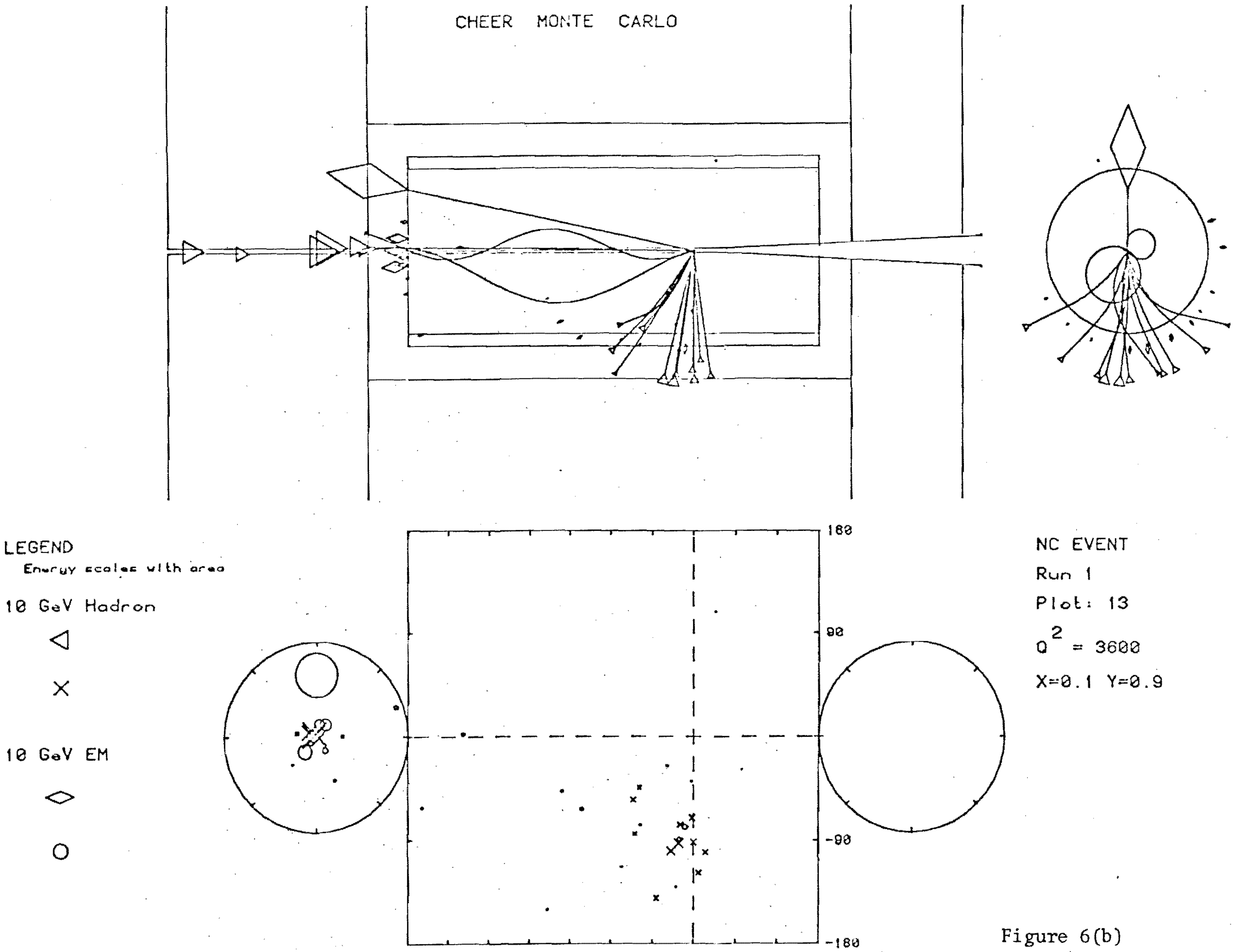
CHEER MONTE CARLO
LEGEND
Energy scales with area
10 GeV Hadron
10 GeV EM
180
90
-90
-180
NC EVENT
Run 1
Plot: 13
Q 2 = 3600
X=0.1 Y=0.9

Figure 6(b)

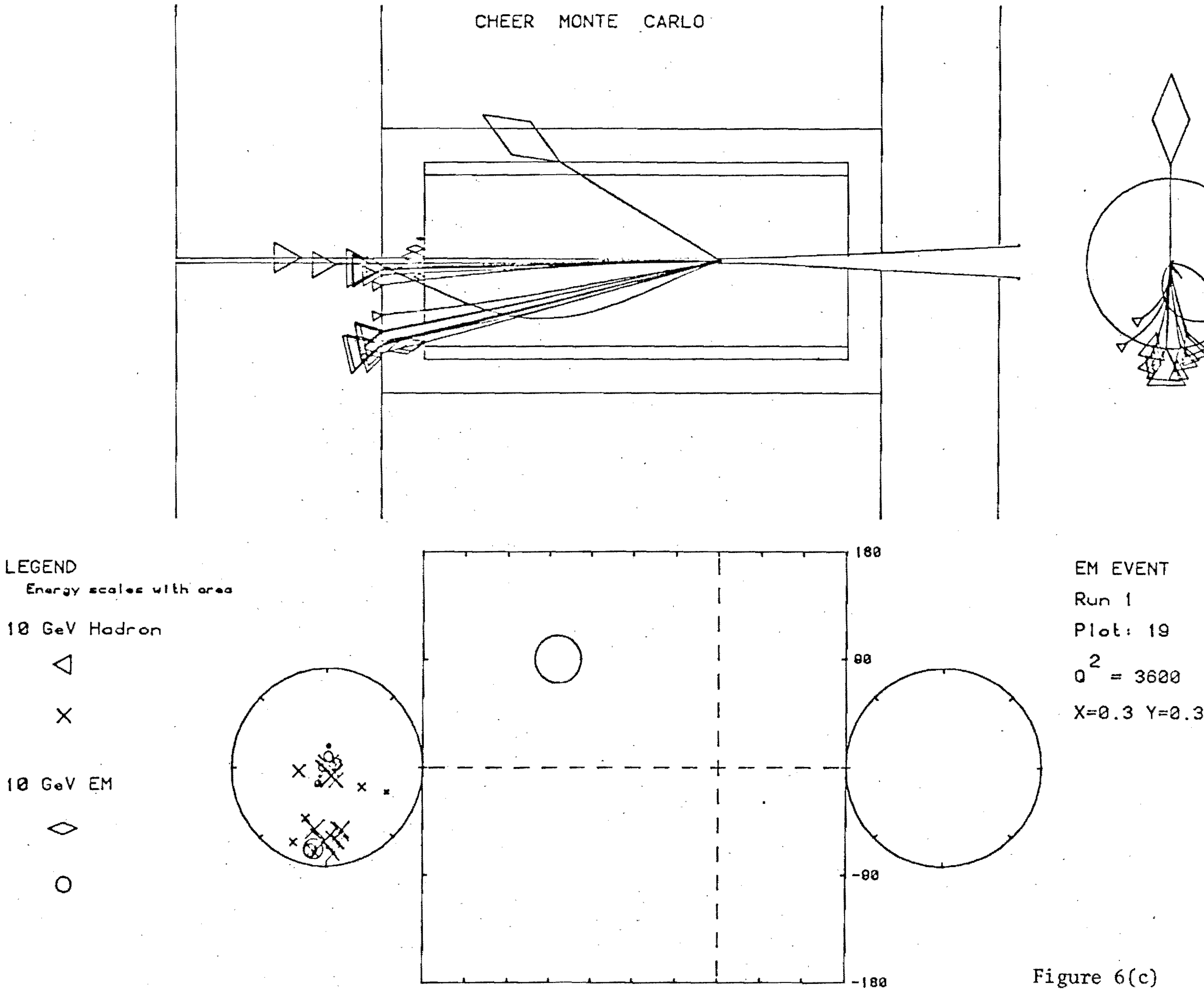
CHEER MONTE CARLO
LEGEND
Energy scales with area
10 GeV Hadron
10 GeV EM
180
90
-90
-180
EM EVENT
Run 1
Plot: 19
Q^2 = 3600
X=0.3 Y=0.3

Figure 6(c)

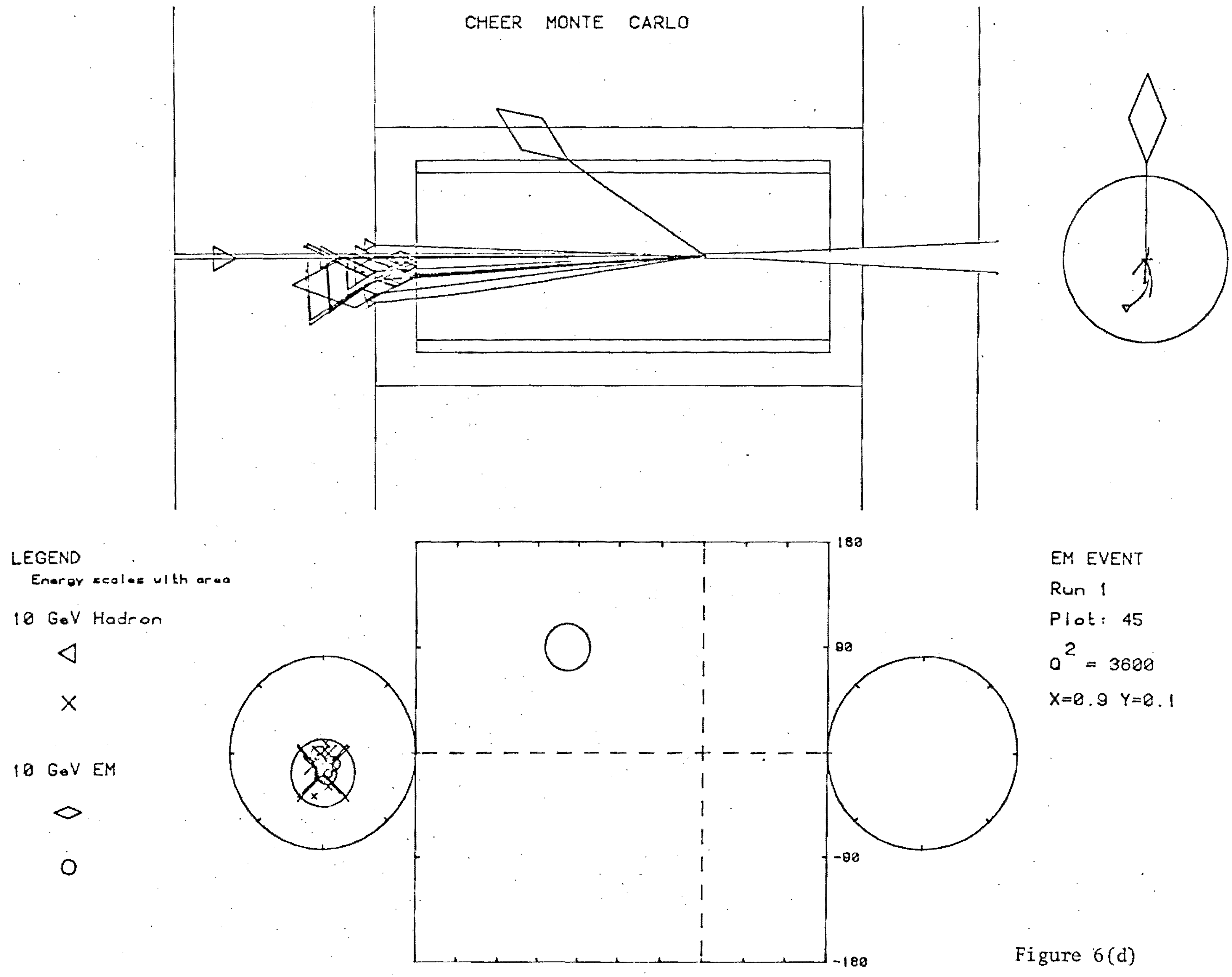
CHEER MONTE CARLO
LEGEND
Energy scales with area
10 GeV Hadron
10 GeV EM
180
90
-90
-180
EM EVENT
Run 1
Plot: 45
Q^2 = 3600
X=0.9 Y=0.1

Figure 6(d)

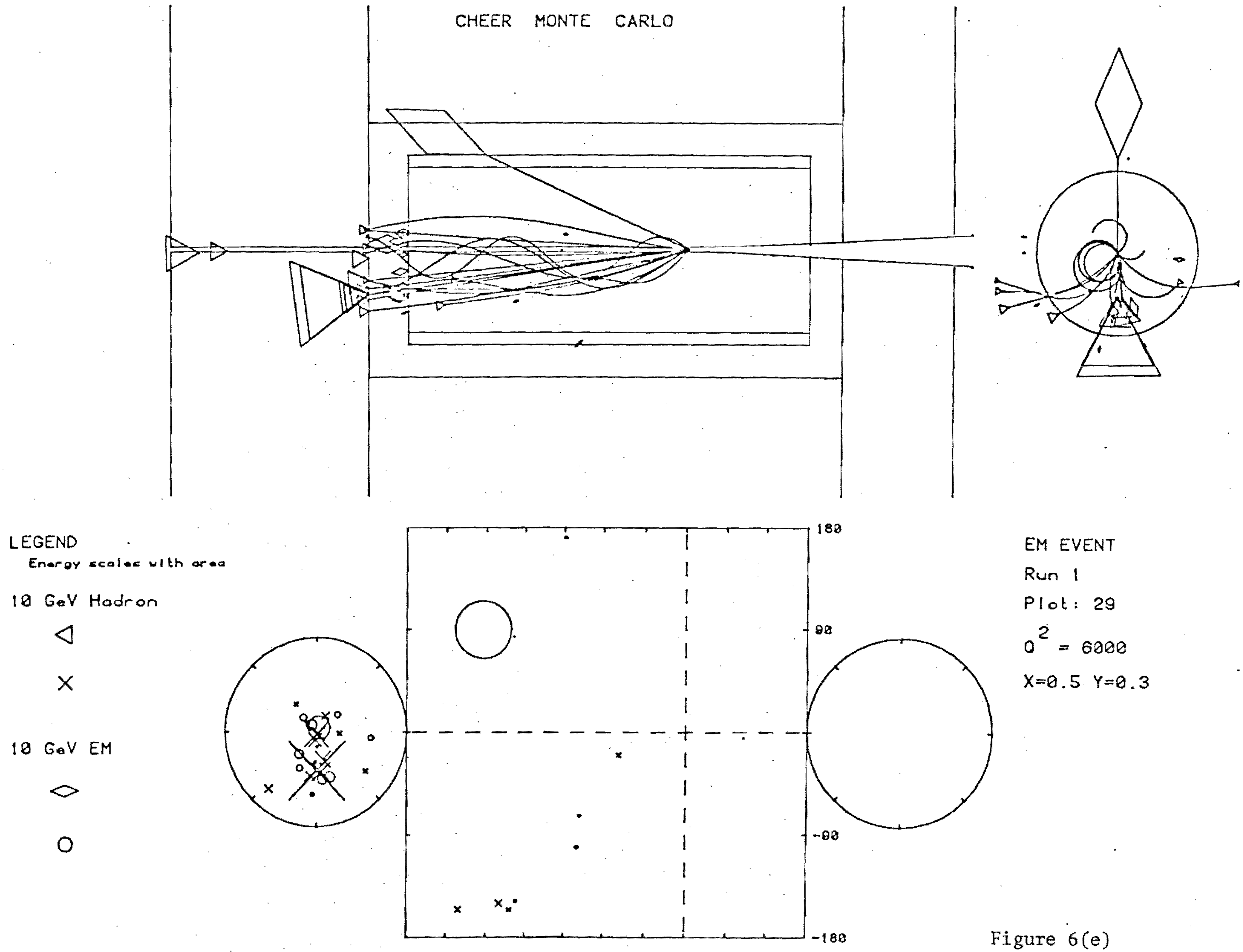
CHEER MONTE CARLO
LEGEND
Energy scales with area
10 GeV Hadron
10 GeV EM
180
90
-90
-180
EM EVENT
Run 1
Plot: 29
Q2 = 6000
X=0.5 Y=0.3

Figure 6(e)

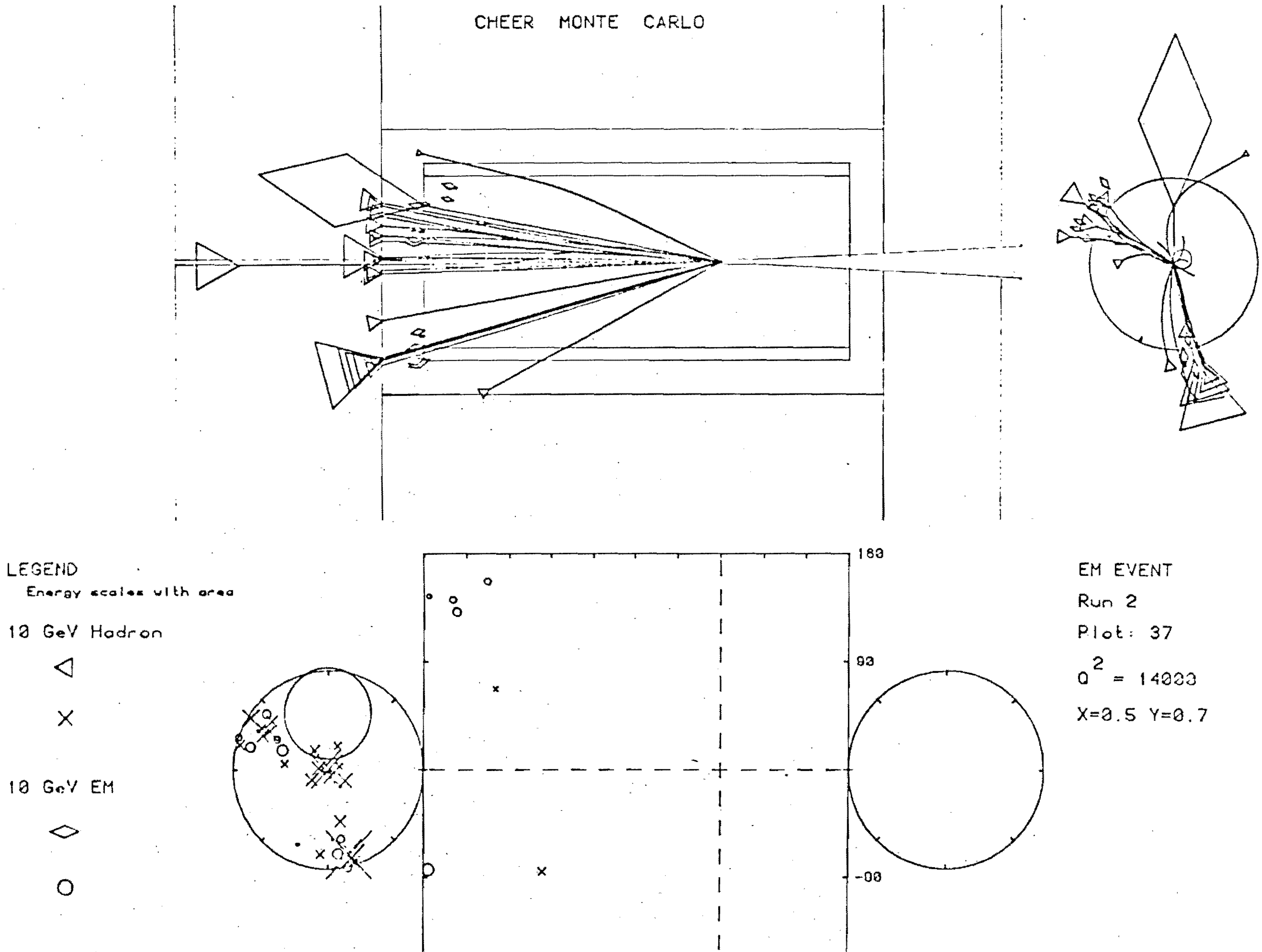
CHEER MONTE CARLO
LEGEND
Energy scales with area
10 GeV Hadron
10 GeV EM
180
90
-90
-180
EM EVENT
Run 2
Plot: 37
Q^2 = 14000
X=0.5 Y=0.7

Figure 6(f)

hadrons. All events are generated to show the final state lepton at "12 o'clock", and trajectories of the hadron jet members are true projections onto that aximuthal plane. The lower half of each figure shows a planar development of the inside surface of the electromagnetic calorimeter showing the point at which it was pierced by each trajectory. Again the areas of the symbols represent the energies of the particles.

III. The Experiment

We now turn to a sketch of the physics that can be extracted from the ep collider and detector we have described. We consider both an initial run of integrated luminosity 4×10^4 nb^{-1} and the data that can be accumulated (over several runs) with an integrated luminosity of 10^6 nb^{-1}.

These integrated luminosities are based on the assumption that it will prove to be possible to commission the electron ring in the by-pass mode: certainly the injection, storage, low β tuning, and polarisation of the electron ring can be brought up in by-pass running. It is also possible that the ep mode can be brought up in parasitic running with the Tevatron operating in a non-ep mode. If so, we can anticipate the above-quoted integrated luminosities from an initial 1000 hour run at about 10^{31} cm^{-2} sec^{-1} and from subsequent runs at constantly improving luminosities that might approach 10^{32} cm^{-2} sec^{-1}, respectively.

The ep collison events recorded by the detector will be rich in physics over an extremely broad kinematic range, from the low Q^2 of photon physics to the high Q^2 of the deep inelastic events. We discuss the data below under various assumed cuts:

1) Deep Inelastic Neutral Current Events

Requiring the observation of a clean electron (i.e., one not buried in a hadron shower) opposite to a hadron jet which balances its p_T is expected to suffice to pull out the deep inelastic neutral current events $e^{\pm}_{L,R}\, p \rightarrow e^{\pm}_{L,R}\, X$. This process can proceed in the standard model by either γ or Z^o exchange and so should exhibit characteristic variations with the charge ($\pm$) and helicity (L,R) of the incident electron, and a characteristic dependence on s and Q^2. This is shown for the representative case of $e^-_L\, p \rightarrow e^-_L\, X$ in Figures 7(a),(b), and (c); similar effects will be evident in the other three channels.

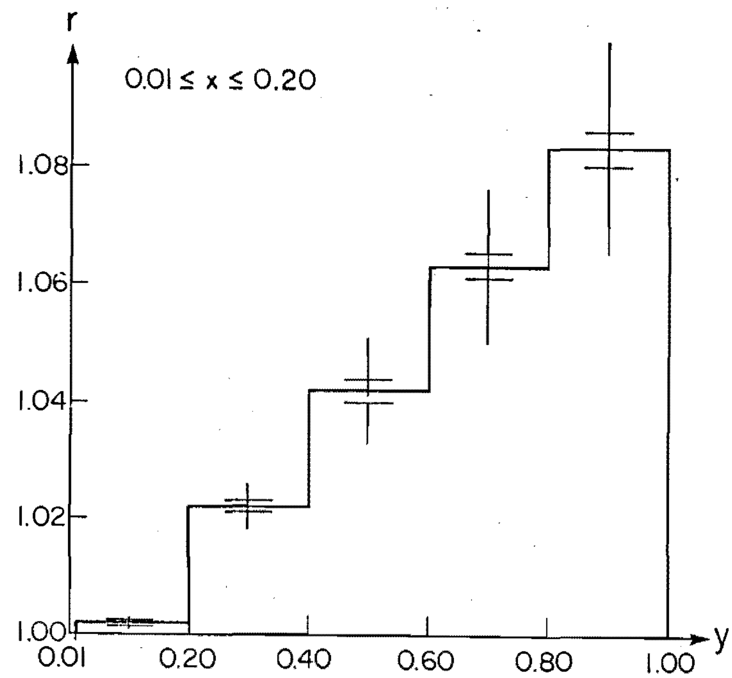

(a)

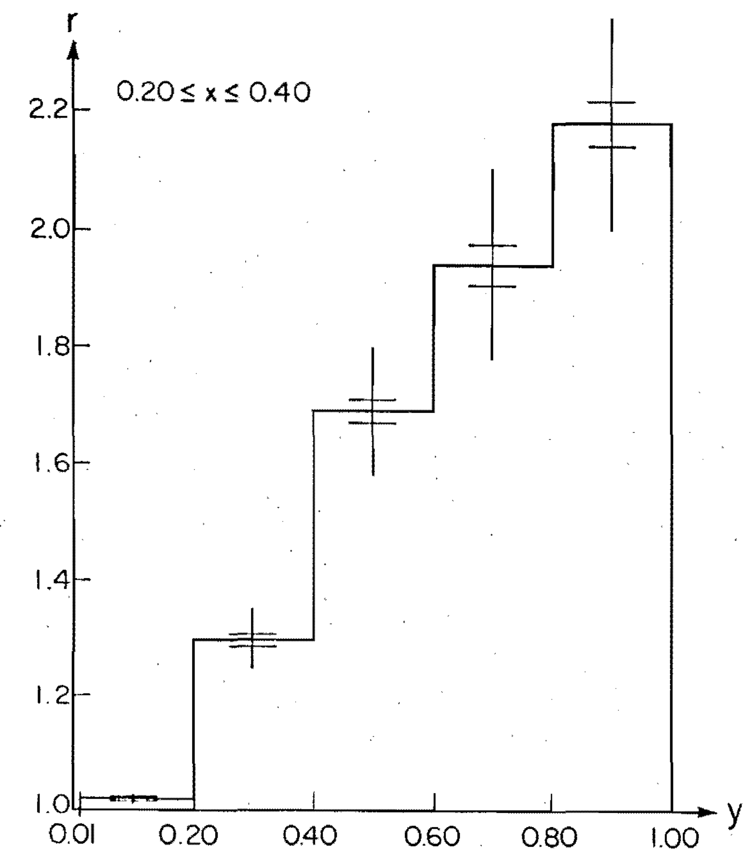

(b)

Figure 7(a): The ratio "r" of the number of events expected in $e^-_L p \to e^-_L X$ to the number expected if the interaction were purely electromagnetic, as a function of y for $0.01 \le x \le 0.20$. The errors shown correspond to the expected statistical fluctuations for integrated luminosities of 4×10^4 nb^{-1} (vertical bars) and 10^6 nb^{-1} (horizontal bars).

(b): As in Figure 7(a), but for $0.20 \le x \le 0.40$.

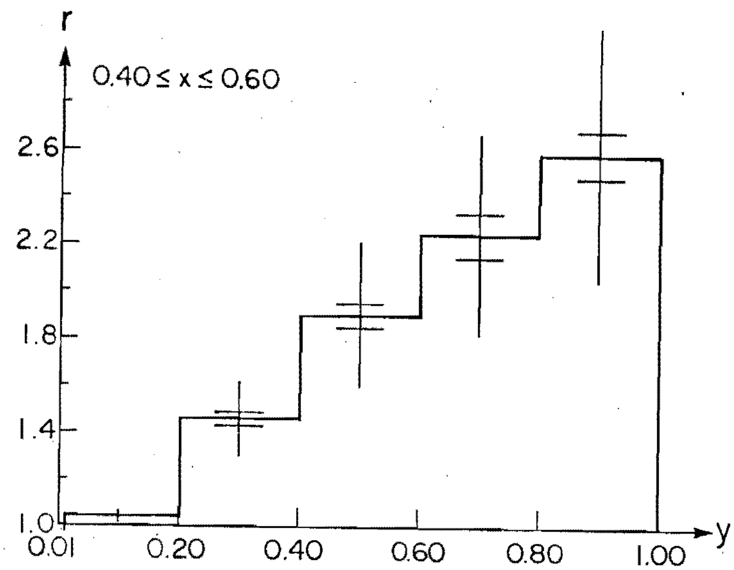

Figure 7(c): As in Figure 7(a), but for $0.40 \leq x \leq 0.60$.

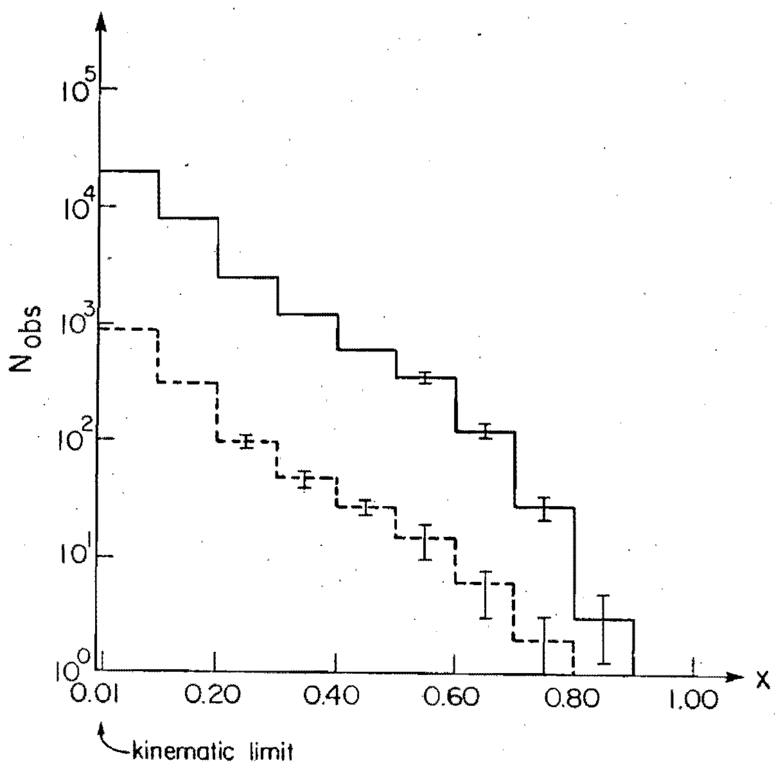

Figure 8(a): The number of events expected in $e^- p \to \nu_e X$ as a function of x for 400 $GeV^2 \leq Q^2 \leq 4{,}000$ GeV^2. The errors shown correspond to the expected statistical fluctuations for integrated luminosities of 4×10^4 nb^{-1} (dashed line) and 10^6 nb^{-1} (solid line); when not indicated, the errors are too small to be shown.

2) Deep Inelastic Charged Current Events

These $e^-p \rightarrow \nu_e X$ events have the characteristics of neutral current events, but with a missing electron, so that a large missing p_T exists opposite to the hadron jet. In Figures 8(a), (b), and (c) we show the number of events of this type expected in the standard model for various ranges of Q^2 in our two hypothetical runs.

In both types of deep inelastic scattering, the most straightforward tests of the standard model will follow from direct comparison of the various measured cross sections with the predicted ones as functions of x, y, s (by varying the proton beam energy), and beam type ($e^{\pm}_{L,R}$). However, these cross sections can also be unravelled to provide measurements of the structure functions, neutral current coupling constants, intermediate boson propagators, etc., that are the components of these predictions. This latter approach will, of course, be the more useful one should any departures from the predicted cross sections be seen. As an illustration of this latter eventuality, consider the possibility that the $W^{\pm}$ mass differs from the standard value: this would appear as an anomalous Q^2 dependence that could be attributed to a propagator effect since it would be independent of x, in contradistinction to readily conceivable structure function effects.

As presented in detail in the Blue Book, the net effect of these studies of deep inelastic events is bound to be profound. If the measured cross sections are all in accord with the standard theory, the effect will be i) to have verified the Glashow-Weinberg-Salam model

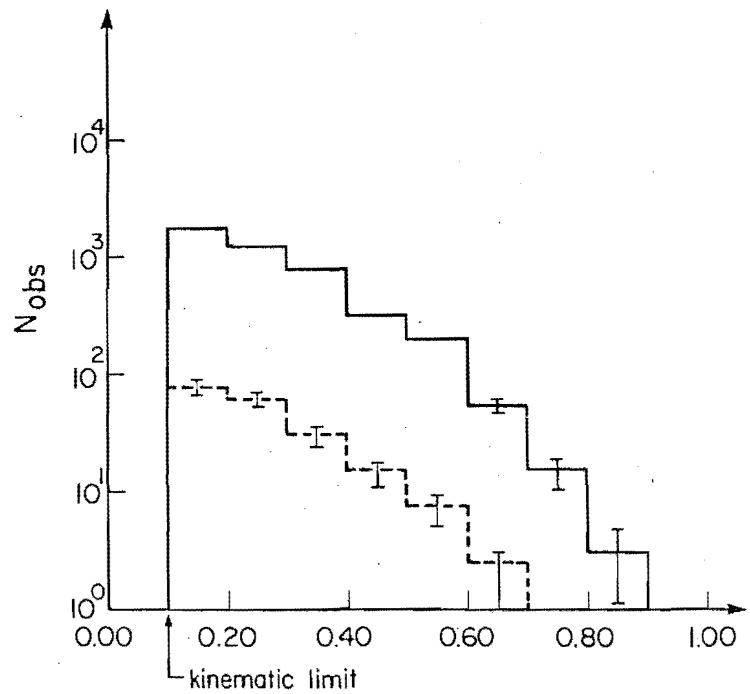

Figure 8(b): As in Figure 8(a), but for 4,000 $GeV^2 \leq Q^2 \leq 10{,}000$ GeV^2.

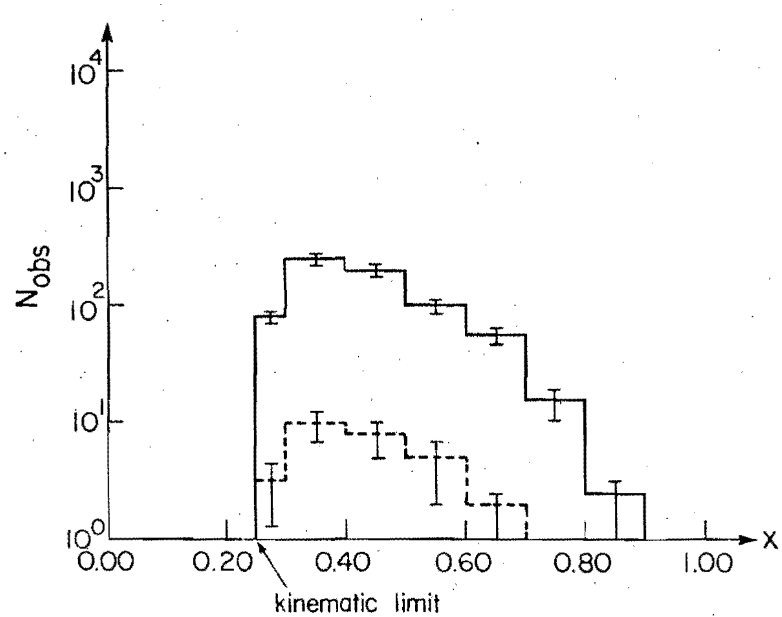

Figure 8(c): As in Figure 8(a), but for $Q^2 > 10{,}000$ GeV^2.

in a new energy regime where the unification of weak and electromagnetic interactions is manifest, ii) to establish QCD as the correct theory of the strong interactions by testing it in the high Q^2 regime where its predictions are rigorous, and iii) to establish (almost coincidentally!) the validity of QED and the elementarity of quarks and leptons in a new spatial domain. On the other hand, should the predictions of the standard theory fail, these studies would lead to the discovery of new phenomena, perhaps already anticipated (the collapse of G-W-S due to extended quark or lepton families or multiple $W^{\pm}$ and Z^{o} bosons, the failure of QCD, the existence of quark and lepton constituents, etc.) but most probably as yet unimagined.

As a final point relevant to the deep inelastic events, we compare the measurements of this type possible with CHEER to those expected in the Tevatron muon beam[6] in Figure 9; the figure demonstrates the great power of CHEER relative to fixed target experiments.

3) Photon Physics

Since the main focus of CHEER is on deep inelastic scattering, it is sometimes forgotten that it will produce a high luminosity photon beam that can be used to explore both short distance phenomena and (via its vector meson component) the hadron-hadron interaction at lab equivalent energies up to 20 TeV. The forward electron tagging detector of CHEER can trigger on millions of γp events per day, even at low initial luminosities. As discussed in more detail in the Blue Book, the photon physics subsample of the CHEER data will provide access to: i) real photon QCD processes like $\gamma p \rightarrow$ high p_T jets, ii) deep inelastic Compton scattering, iii) pair production of heavy quarks with masses up to $2M_q \simeq 100$ GeV, iv) $\sigma_{\gamma p}(\nu)$ up to $\nu = 20$ TeV, v) diffractive photoproduction of vector mesons and the Primakoff production of even C states, vi) eleastic Compton scattering, vii) photon fragmentation, and many other processes too numerous to mention. Monte Carlo studies are now underway to maximize

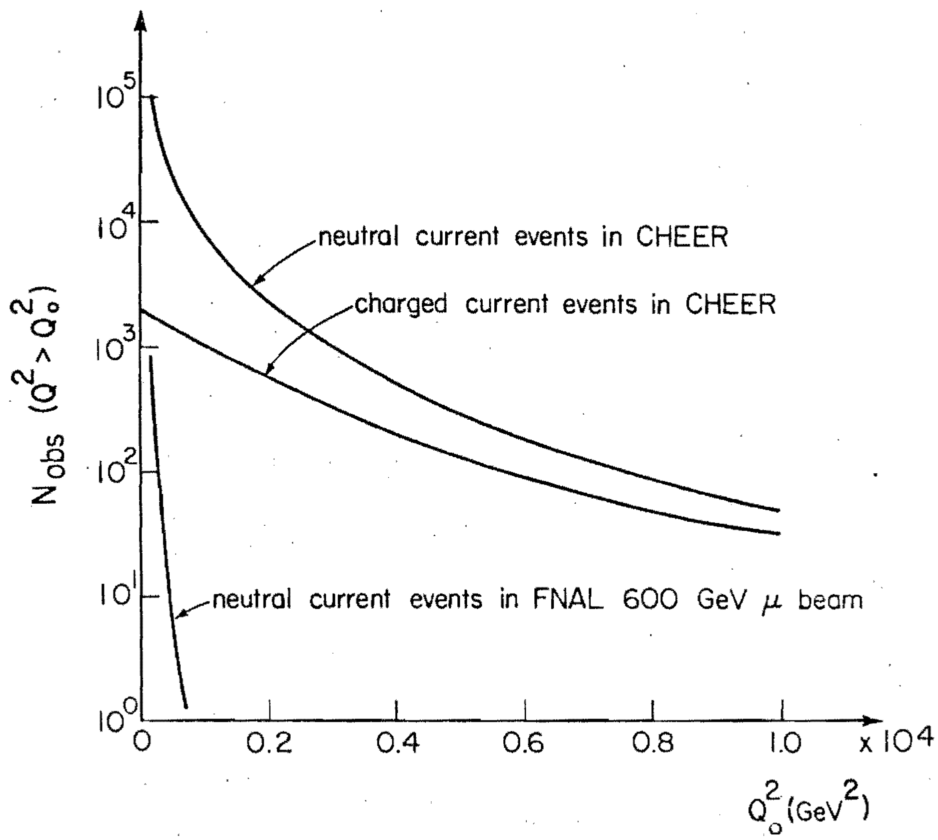

Figure 9: A comparison between the number of events expected with $Q^2 > Q_o^2$ in CHEER and the Tevatron muon beam during 1000 hours of initial running. For CHEER this corresponds to 1000 hours at a luminosity of 10^{31} cm^{-2}sec^{-1}; for the muon beam to 2.2×10^{12} muons on a 1.0 metre H_2 target.

the efficiency of the CHEER detector for studying these processes.

4) Other Physics

As discussed in the Blue Book, it is possible to study many other phenomena with CHEER. Monte Carlo simulations are necessary to adequately assess the feasibility of such studies, but we believe that among them will be (if we assume the standard picture holds) i) the measurement of multiple jet cross sections and jet broadening, ii) the study of the fragmentation functions of u and d quarks and their Q^2 dependence, iii) the measurement of the Kobayashi-Maskawa angles for u $\leftrightarrow$ b transitions, and iv) the study of the colour hadronisation process.

5) New Physics

In the event that the standard picture fails, the programme for CHEER will be contingent on how it fails. We can nevertheless anticipate that in such circumstances, as in the past, ep collisions would provide the best probe available into the new physics being discovered.

IV. Acknowledgements

The CHEER Group gratefully acknowledes the assistance of many people not listed on the cover page of this proposal. Certainly we thank those who contributed to the studies which have preceded this proposal, including K. Anderson, G. Bancroft, D. Beder, J. Buon, B. Campbell, E. Courant, G. Danby, V. Elias,D. Gurd, M. Harrison, M. Harvey, S. Holmes, G. Ingelman, P. Jackson, J. Jovanovich, C.S. Kalman, A.N. Kamal, G. Karl, L.Krauss, D. Laughton, H.C. Lee, W. McGowan, G. McKeon, R. Migneron, J.B. Mitchell, B.W. Montague, B. Norum, C. Pellegrini, H.K. Quang, Y.M. Shin, I. Stumer, M.K. Sundaresan, P.J.S. Watson, E. Williams and S. Wipf. The CHEER group would especially like to acknowledge E. Courant for the use of his thick lens version of the program SLIM. Finally, we would like to recognise the role played by R.J. Hemingway as chairman of the CHEER Project during the preparation of the feasibility study.

V. References

1. CHEER: A Feasibility Study for an Electron Ring at a High Energy Proton Accelerator, I.P.P. Report, September, 1980.
2. Fermilab Proposal 659: Electron-Proton Interaction Experiment.
3. I.E.E.E. Transactions on Nuclear Science, NS-26, 3244(1979).
4. F. Jacquet and A. Blondel, DESY report 79/48.
5. G. Ingelman and T. Sjostrand, Lund preprint LU TP 80-12.
6. Fermilab Proposal   : Muon Scattering with Hadron Detection at the Tevatron.